Cherish every Joule: Maximizing throughput with an eye on network-wide energy consumption

Canming Jiang   Yi Shi   Y. Thomas Hou   Wenjing Lou

Virginia Polytechnic Institute and State University, USA

Email: {jcm, yshi, thou, wjlou}@vt.edu

Abstract

Conserving network-wide energy consumption is becoming an increasingly important concern for network operators. In this work, we study network-wide energy conservation problem which we hope will offer insights to both network operators and users. In the first part of this work, we study how to maximize throughput under a network-wide energy constraint. We formulate this problem as a mixed-integer nonlinear program (MINLP). We propose a novel piece-wise linear approximation to transform the nonlinear constraints into linear constraints. We prove that the solution developed under this approach is near-optimal with guaranteed performance bound. In the second part, we generalize the problem in the first part by exploring throughput and network-wide energy optimization via a multicriteria optimization framework. We show that the weakly Pareto-optimal points in the solution can characterize an optimal throughput-energy curve. We offer some interesting properties of the optimal throughput-energy curve which are useful to both network operators and end users.

Keywords

Network-wide energy, network throughput, optimization, multicriteria optimization, multi-hop wireless networks

1 Introduction

With the proliferation of wireless networks, the concern of energy consumption is becoming increasingly important for network operators. Conserving network-wide energy consumption not only can help reducing CO_2 emissions and protect the environment, but also can significantly reduce the operating cost for network providers. Since energy-related operating cost is directly tied to *network-wide* energy consumption, it is critical to study network optimization problems with an eye on total network-wide energy consumption.

In this paper, we study network-wide energy conservation problem in a multi-hop wireless network which we hope will offer insights to both network operators and end users. Specifically, in the first part of this work, we will show how to maximize network throughput under a given network-wide total energy consumption budget. This may correspond to a scenario where a network operator has a budget on total energy consumption. In the second part, we generalize the problem in the first part by studying how to optimize both network throughput and network-wide energy consumption through a multicriteria optimization framework. This allows us to characterize the trend of throughput when the total energy consumption budget changes.

We recognize that there is a wealth of literature on optimizing network throughput with energy considerations. A major branch of these prior efforts followed various heuristic approaches in developing physical, link, and network layer schemes and algorithms (see, e.g., [20, 22]). This is in contrast to our work in this paper, which follows a formal optimization framework with the goal of offering performance guarantee of the final solution.

Within the branch of related work that followed formal optimization framework in studying network throughput maximization with energy consideration (see, e.g., [8, 19]), we find that most of these works only considered per-link power constraint or per-node power constraint. Although these constraints are important to characterize local energy consumption, it is not clear how to extend results for local link/node energy conservation to *network-wide* energy conservation, due to the complex inter-dependencies among the layers. Therefore, these prior results cannot directly benefit network operators, who are more concerned with total network-wide energy consumption.

Our work is complementary to a branch of previous work that addressed how to minimize network-wide energy consumption while satisfying some traffic demands (see, e.g., [14, 17]). These works are orthogonal to the problem that we shall study in the first part of this paper. It will soon be clear that our mathematical formulation and proposed solution differ from all these seemingly similar efforts. Further, in the second part of this paper, we consider joint optimization of throughput and network-wide energy, which explores the domain of multi-criteria optimization that is not well studied in the wireless networking community. In our recent work in [11], we explored multicriteria optimization of network energy and throughput. However, power control was not considered in [11]. In this work, we shall consider power control at each node, which is more interesting.

The main contributions of this paper are the following:

- First, we study how to maximize network throughput under a total network-wide energy consumption constraint. We show that this problem involves both network and physical layer variables and can be formulated as a mixed-integer nonlinear program (MINLP). To solve this problem efficiently, we propose a novel piece-wise linear approximation to transform the nonlinear constraints into linear constraints. We prove that the solution developed under this linear approximation is near-optimal in the sense that the performance gap between our solution and the optimal solution (despite unknown) can be made arbitrary narrow depending on required accuracy.

- Second, we generalize the problem in the first part by exploring joint optimization of both network throughput and network energy consumption via a multicriteria optimization framework, i.e., *maximizing* network throughput while *minimizing* network-wide energy consumption. We find that all the weakly Pareto-optimal points characterize an optimal throughput-energy curve. This curve shows how the maximum network throughput changes as total network-wide energy budget changes. We offer some interesting properties of this optimal throughput-energy curve that are useful to both network operators and end users.

The remainder of this paper is organized as follows. In Section 2, we describe our network model. In Section 3, we study how to maximize network throughput under a given total network-wide energy budget. In Section 4, we study how to optimize both network throughout and energy under a multicriteria framework. Section 5 presents some numerical results that illustrate our theoretical findings. Section 6 concludes this paper.

2 Network Model

Consider a multi-hop wireless ad hoc network, represented by a directed graph $\mathcal{G} = \{\mathcal{N}, \mathcal{L}\}$, where $\mathcal{N}$ and $\mathcal{L}$ are the sets of nodes and directional links, respectively. A link between two nodes exists if and only if the distance between the two is within a certain transmission range. If two nodes are not within one-hop of each other, then a node has to resort to multi-hop to relay messages. We

Table 1: Notation.

Symbol	Definition
B_l	Channel bandwidth on link l
c_l	Capacity of link l
d_l	Distance between link l's transmitting node and receiving node
$d(f)$	Destination node of session $f \in \mathcal{F}$
$\mathcal{F}$	The set of user sessions in the network
h_l	Channel gain on link l
$\mathcal{L}$	The set of links in the network
$\mathcal{L}_i^{\text{In}}$	The set of incoming links at node i
$\mathcal{L}_i^{\text{Out}}$	The set of outgoing links at node i
$\mathcal{N}$	The set of nodes in the network
p_l	Transmission power of link l
P_d	The circuits power consumption of an active link
P	$= \sum_{l \in \mathcal{L}} (p_l + y_l P_d)$, network-wide energy consumption rate
P_{net}	Network-wide energy budget
$r(f)$	Data rate of session $f \in \mathcal{F}$
$r_l(f)$	Data rate on link l that is attributed to session f
$s(f)$	Source node of session f
U	$= \sum_{m \in \mathcal{M}} w(f) r(f)$, the network throughput
$w(f)$	A weight assigned to session $f \in \mathcal{F}$
y_l	A binary variable indicating whether or not link l is active
η	Ambient Gaussian noise density

assume orthogonal channels on all links (similar to that in [2, 13, 15]). This can be done by some interference avoidance mechanism (e.g., OFDMA). Note that orthogonal channels do not require as many channels as the number of active links in the network since one can reuse channels on links that are spatially far away from each other. This is called spatial reuse and is commonly used in wireless networks to improve channel efficiency. Note that designing a channel assignment algorithm to achieve orthogonality has been well studied in the literature and its discussion is beyond the scope of this paper.

We assume there is a set of $\mathcal{F}$ active (unicast) communication sessions in the network. Denote $s(f)$ and $d(f)$ the source and destination nodes of session $f \in \mathcal{F}$, respectively. To differentiate the importance of these user sessions, each session f is assigned a weight $w(f)$. Denote $r(f)$ the data rate of session f. The network throughput U in this paper is represented by the sum of weighted session rates, which is $\sum_{f \in \mathcal{F}} w(f) \cdot r(f)$. Table 1 lists all the notation in this paper.

2.1 Energy Consumption and Power Control

When a wireless link is active for communications, its energy consumption includes transmission power and device power [4, 16], where transmission power is for data transmission over a distance and device power is consumed by device electronics for encoding, modulation, decoding, demodulation, etc. Denote P_d as device power, which we assume is a constant if link is active. Denote p_l the transmission power on link l, which is a tunable (variable) system parameter.

Denote y_l a binary variable indicating whether or not link l is active, i.e.,

$$y_l = \begin{cases} 1 & \text{if link } l \text{ is active;} \\ 0 & \text{otherwise.} \end{cases}$$

The energy consumption rate of link l, including transmission power and device power, is $p_l + y_l P_d$.

Assume that the maximum transmission power of a node is $P_{\max}$. Then, we have the following relationship between p_l and y_l:

$$p_l \le y_l \cdot P_{\max} \quad (l \in \mathcal{L}) \ . \tag{1}$$

For all active links at a node, we have the following node-level transmission power constraint:

$$\sum_{l \in \mathcal{L}_i^{\text{Out}}} p_l \le P_{\max} \quad (i \in \mathcal{N}) \ , \tag{2}$$

where $\mathcal{L}_i^{\text{Out}}$ is the set of potential outgoing links at node i.

Denote P as the total energy consumption rate on all active links in the network. Then, the network-wide energy consumption rate P can be written as $P = \sum_{l \in \mathcal{L}} (p_l + y_l P_d)$.

2.2 Routing and Link Capacity

To transport data from a source node to its destination node that is more than one-hop away, multi-hop relaying is necessary. Since single-path flow routing is overly restrictive and is unlikely to offer optimal solution, we allow flow splitting so that data can be delivered on multi-path routes. We model multi-path flow routing as follows. Denote $r_l(f)$ the amount of flow rate on link l that is attributed to session $f \in \mathcal{F}$. Denote $\mathcal{L}_i^{\text{In}}$ the set of potential incoming links at node i. If node i

is the source node of session f, i.e., $i = s(f)$, then

$$\sum_{l \in \mathcal{L}_i^{\mathrm{Out}}} r_l(f) = r(f) \ . \tag{3}$$

If node i is an intermediate relay node of session f, i.e., $i \neq s(f)$ and $i \neq d(f)$, then

$$\sum_{l \in \mathcal{L}_i^{\mathrm{Out}}}^{l \neq (i, s(f))} r_l(f) = \sum_{m \in \mathcal{L}_i^{\mathrm{In}}}^{m \neq (d(f), i)} r_m(f) \ . \tag{4}$$

If node i is the destination node of session f, i.e., $i = d(f)$, then

$$\sum_{l \in \mathcal{L}_i^{\mathrm{In}}} r_l(f) = r(f) \ . \tag{5}$$

It can be easily verified that if (3) and (4) are satisfied, then (5) must be satisfied. As a result, it is sufficient to list only (3) and (4) in the formulation.

Under the above flow routing scheme, the aggregate flow rate at link l is $\sum_{f \in \mathcal{F}} r_l(f)$. Since aggregate flow rate on any link cannot exceed the link's capacity, we have the following link capacity constraint:

$$\sum_{f \in \mathcal{F}} r_l(f) \leq c_l \quad (l \in \mathcal{L}) \ , \tag{6}$$

where c_l is the capacity on link l. Given that we are employing orthogonal channels among the links in the network, we have:

$$c_l = B_l \log_2 (1 + \frac{p_l \cdot h_l}{\eta B_l}) \ , \tag{7}$$

where B_l is the bandwidth of link l under a given channel assignment, h_l is channel gain between the transmitter and receiver of link l and η is the ambient Gaussian noise density. Combining (6) and (7), we have:

$$\sum_{f \in \mathcal{F}} r_l(f) \leq B_l \log_2 (1 + \frac{p_l \cdot h_l}{\eta B_l}) \quad (l \in \mathcal{L}) \ . \tag{8}$$

Note that constraint (8) couples network flow variables (i.e., $r_l(f)$) and physical layer power variable p_l.

3 Throughput Maximization Under Network-wide Energy Constraint

In this section, we study how to maximize network throughput under a given network-wide energy budget. This problem is motivated by the scenario where we have a strict total energy consumption limit in the network (e.g., due to a given operating budget on energy). The question that we pose is: Given the network-wide energy operating budget P_{net}, i.e.,

$$P = \sum_{l \in \mathcal{L}} (p_l + y_l P_d) \leq P_{\text{net}}, \tag{9}$$

how to adjust the power on each link and multi-path routing for each session so that the maximum network throughput is achieved?

Mathematically, this problem can be formulated as follows:

$$\begin{aligned}
\textbf{OPT:} \quad \max \quad & U = \sum_{f \in \mathcal{F}} w(f) r(f) \\
\text{s.t.} \quad & \text{Constraints } (1), (2), (3), (4), (8), (9) \\
& \text{Variables } y_l \in \{0, 1\}, p_l, r_l(f), r(f) \geq 0 \ (l \in \mathcal{L}, f \in \mathcal{F}) \ ,
\end{aligned}$$

where y_l is a binary variable, p_l, $r(f)$ and $r_l(f)$ are continuous variables and all the other parameters are constants. OPT is a mixed-integer nonlinear program (MINLP), which in general is NP-hard [9]. Note that the network-wide energy constraint complicates overall problem by bringing in integer variables.

MINLP problems are known to be difficult due to the combinatorial nature of mixed integer programs and the difficulty in solving nonlinear programs. Note that there exist some techniques to address *general* MINLP problems (e.g., outer approximation methods [6], branch-and-bound [7], extended cutting plane methods [21], and generalized Benders' decomposition [10]). But these techniques do not exploit our problem-specific structures and properties, and hence can only handle small-size problems.

In this paper, we exploit the structure of our MINLP problem and develop a novel near-optimal solution with performance guarantee. Note that in OPT's formulation, the only set of nonlinear

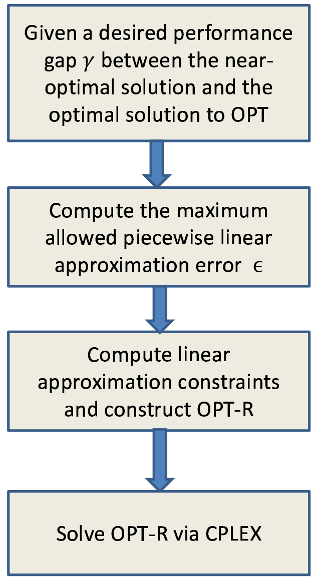

Figure 1: A flow chart to develop a near-optimal solution to OPT.

constraints are the link capacity constraints in (8), which involve the $\log$ function. To address this problem, we propose a piece-wise linear approximation technique to transform the nonlinear constraints to linear constraints. Our main idea is as follows. We first use a set of linear segments to approximate the $\log$ term in (8) and guarantee the linear approximation error will not exceed a threshold ϵ. Subsequently, the nonlinear constraints in OPT are replaced by a set of linear constraints. Denote the linearized optimization problem as OPT-R, which is a MILP problem. Since MILP problems are much easier than MINLP problems, we can apply a solver such as CPLEX [3] to obtain a solution efficiently.

We will show that solving OPT-R can give us a near-optimal solution to the original problem OPT. Denote γ as desired performance gap of our near-optimal solution, i.e., the difference in the objective values between the optimal solution and the near-optimal solution to OPT. We analyze the relationship between performance gap γ and the linear approximation error ϵ (see details in Section 3.2). Specifically, for a desired performance gap γ, we compute the maximum allowed linear approximation error ϵ. After obtaining ϵ, we can compute the linear approximation constraints and construct OPT-R (see details in Section 3.1). Solving the OPT-R will give us a near-optimal solution with performance guarantee γ. We summarize the above steps in Fig. 1. In the rest of this section, we fill in the details of these steps.

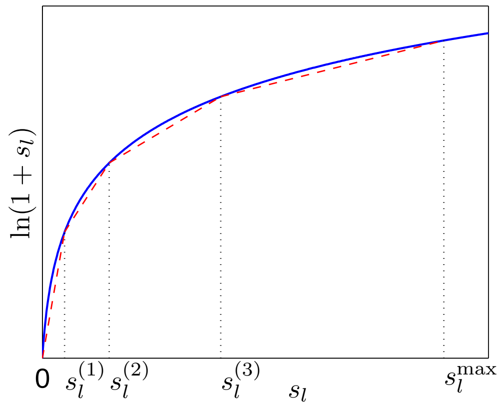

Figure 2: An illustration of piece-wise linear approximation with four linear segments.

3.1 Piece-wise Linear Approximation

The nonlinear constraint in (8) can be written as

$$\sum_{f \in \mathcal{F}} r_l(f) \leq \frac{B_l}{\ln 2} \ln(1 + \frac{p_l \cdot h_l}{\eta B_l}). \tag{10}$$

To simplify notation, denote

$$s_l = \frac{p_l h_l}{\eta B_l} \ . \tag{11}$$

Then, the nonlinear term in (10) can be written as $\ln(1+s_l)$. The range of s_l is $[0, s_l^{\max}]$, with $s_l^{\max} = (P_{\max} h_l)/(\eta B_l)$. Our piece-wise linear approximation is to use a set of consecutive linear segments to approximate $\ln(1+s_l)$ for $s_l \in [0, s_l^{\max}]$ (see Fig. 2). Denote ϵ the maximum allowed error of this linear approximation. Denote K_l the number of linear segments that is needed to meet this error requirement. (K_l will be determined later.) Denote $s_{l,0}, s_{l,1}, \ldots, s_{l,K_l}$ the X-axis values of the endpoints of these K segments, with $s_{l,0} = 0$ and $s_{l,K_l} = s_l^{\max}$.

A naive approach to generate a linear approximation is making $s_l^{(k)}, k = 0, \ldots, K_l$, evenly distributed between $[0, s_l^{\max}]$. When setting K_l sufficiently large, the linear approximation error requirement will be satisfied. Although this approach is straightforward and easy to implement, it will generate too many linear segments to approximate $\ln(1+s_l)$. Note that the derivative of curve $\ln(1+s_l)$ decreases as s_l increases. This motivates us to enlarge the size of an interval as s_l increases. Thus, we want to pursue an algorithm that optimally divides the K_l intervals within $[0, s_l^{\max}]$. By "optimally", we refer to finding the *minimum* K_l such that the maximum approximation error of each line segment is no more than ϵ.

Denote $m_l^{(k)}$ as the slope of the k-th linear segment, i.e.,

$$m_l^{(k)} = \frac{\ln(1+s_l^{(k)}) - \ln(1+s_l^{(k-1)})}{s_l^{(k)} - s_l^{(k-1)}}. \tag{12}$$

Denote $g_l^{(k)}(s_l)$ as the k-th linear approximation segment (see Fig. 3), which can be represented as follows:

$$g_l^{(k)}(s_l) = m_l^{(k)} \cdot \left(s_l - s_l^{(k-1)}\right) + \ln\left(1 + s_l^{(k-1)}\right), \text{ for } s_l^{(k-1)} \le s_l \le s_l^{(k)}. \tag{13}$$

Our algorithm computes the values of $s_l^{(0)}, \ldots, s_l^{(K_l)}$ sequentially (for a given ϵ) based on Algorithm 1 as follows.

Algorithm 1 *Initialization:* $k := 0$ *and* $s_l^{(0)} := 0$.

1. $k := k + 1$.
2. *Compute* $m_l^{(k)}$ *satisfying*

$$-\ln(m_l^{(k)}) + m_l^{(k)}(1 + s_l^{(k-1)}) - 1 - \ln(1 + s_l^{(k-1)}) = \epsilon. \tag{14}$$

3. *After obtaining* $m_l^{(k)}$*, compute* $s_l^{(k)}$ *satisfying (12).*
4. *If* $s_l^{(k)} < s_l^{\max}$*, go back to Step 1.*
5. $K_l := k$*;* $s_l^{(K_l)} := s_l^{\max}$.
6. *Update* $m_l^{(K_l)}$ *using (12).*

The values of $m_l^{(k)}$ in (14) and $s_l^{(k)}$ in (12) can be solved by numerical methods such as bisection method or Newton's method [18, Chapter 2].

Our linear approximation method (Algorithm 1) satisfies the linear approximation error requirement with the minimum number of linear segments to approximate $\ln(1+s_l)$ for $s_l \in [0, s_l^{\max}]$. We formalize these two claims in the following two lemmas.

Lemma 1 *For the piece-wise linear approximation generated by Algorithm 1, the maximum approximation error of each linear segment is at most* ϵ.

Proof Denote $\epsilon_l^{(k)}$ the maximum linear approximation error for the k-th linear segment, i.e.,

$$\epsilon_l^{(k)} = \max_{s_l^{(k-1)} \leq s_l \leq s_l^{(k)}} \left| \ln(1+s_l) - g_l^{(k)}(s_l) \right| = \max_{s_l^{(k-1)} \leq s_l \leq s_l^{(k)}} \left\{ \ln(1+s_l) - g_l^{(k)}(s_l) \right\},$$

where the equality holds since $\ln(1+s_l)$ is a convex function of s_l and all linear segments lie beneath the $\ln(1+s_l)$ curve.

Consider the k-th linear segment. Referring to Fig. 3, we can move $g_l^{(k)}(s_l)$ upward until it is tangential to the $\ln(1+s_l)$ curve. It is easy to see that the tangential point achieves the maximum approximation error $\epsilon_l^{(k)}$. Denote $\hat{s}_l^{(k)}$ the X-axis value of that tangential point. Since the derivative of $\ln(1+s_l)$ is $\frac{1}{1+s_l}$, we have $\frac{1}{1+\hat{s}_l^{(k)}} = m_l^{(k)}$, i.e,

$$\hat{s}_l^{(k)} = \frac{1}{m_l^{(k)}} - 1, \tag{15}$$

where $m_l^{(k)}$ is slope of linear segment $g_l^{(k)}(s_l)$. Therefore, the maximum approximation error $\epsilon_l^{(k)}$ can be written as

$$\begin{aligned}
\epsilon_l^{(k)} &= \ln(1+\hat{s}_l^{(k)}) - g_l^{(k)}(\hat{s}_l^{(k)}) = \ln(1+\hat{s}_l^{(k)}) - [m_l^{(k)} \cdot (\hat{s}_l^{(k)} - s_l^{(k-1)}) + \ln(1+s_l^{(k-1)})] \\
&= \ln\left(1 + \frac{1}{m_l^{(k)}} - 1\right) - \left\{ m_l^{(k)} \cdot \left[\frac{1}{m_l^{(k)}} - 1 - s_l^{(k-1)}\right] + \ln(1+s_l^{(k-1)}) \right\} \\
&= -\ln(m_l^{(k)}) + m_l^{(k)}(1+s_l^{(k-1)}) - 1 - \ln(1+s_l^{(k-1)}),
\end{aligned}$$

where the second equality holds due to (13) and the third equality holds due to (15).

In Algorithm 1, we set $-\ln(m_l^{(k)}) + m_l^{(k)}(1+s_l^{(k-1)}) - 1 - \ln(1+s_l^{(k-1)}) = \epsilon$. Thus, the maximum linear approximation error for the k-th linear segment is ϵ. This result holds for all $k = 1, \cdots, K_l$. This completes the proof. $\square$

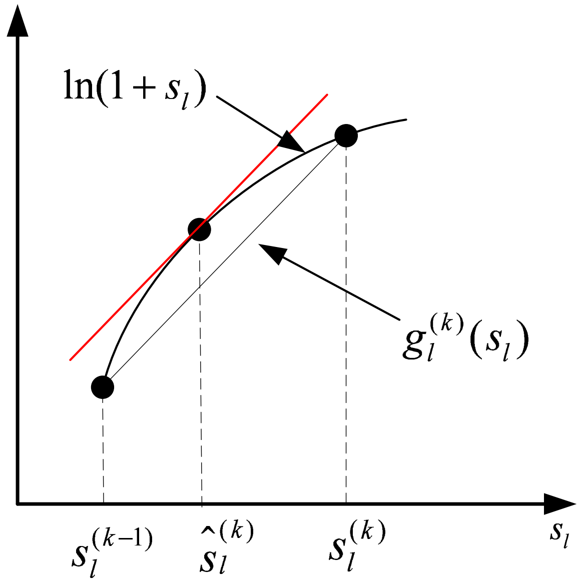

Figure 3: An illustration of the maximum approximation error for the k-th linear segment.

Lemma 2 *For a given approximation error bound ϵ for each linear segment, the number of linear segments to approximate $\ln(1+s_l)$ for $s_l \in [0, s_l^{\max}]$ is minimized by Algorithm 1.*

The proof of Lemma 2 is given in the appendix.

With the proposed piece-wise linear approximation of $\ln(1+s_l)$, constraint (8) can be replaced by the following set of constraints:

$$\sum_{f \in \mathcal{F}} r_l(f) \leq \frac{B_l}{\ln 2} g_l^{(k)}(s_l) \qquad (k = 1, \ldots, K_l, l \in \mathcal{L}) \ ,$$

where s_l and $g_l^{(k)}(s_l)$ are given in (11) and (13), respectively. Substituting (11) and (13) into the above equation, we have

$$\sum_{f \in \mathcal{F}} r_l(f) \leq \frac{B_l}{\ln 2} \left\{ m_l^{(k)} \left[\frac{p_l h_l}{\eta B_l} - s_l^{(k-1)} \right] + \ln \left[1 + s_l^{(k-1)} \right] \right\} \quad (k = 1, \ldots, K_l, l \in \mathcal{L}) \ . \quad (16)$$

By replacing the nonlinear constraints in (8) with the set of linear constraints in (16), we have a revised formulation for OPT, which we denote as OPT-R.

$$\textbf{OPT-R:} \quad \max \sum_{f\in\mathcal{F}} w(f)r(f)$$
$$\text{s.t.} \quad \text{Constraints } (1), (2), (3), (4), (9), (16)$$
$$\text{Variables } y_l \in \{0,1\}, p_l, r_l(f), r(f) \geq 0 \ (l \in \mathcal{L}, f \in \mathcal{F}) \ .$$

We have the following lemma on the relationship between OPT-R and OPT. Its proof is given in the appendix.

Lemma 3 *A feasible solution to OPT-R is a feasible solution to OPT.*

3.2 A Near-Optimal Solution

OPT-R is a mixed-integer linear program (MILP) and can be solved efficiently by CPLEX solver [3]. Now we give a bound for the gap between the optimal objective values of OPT and OPT-R, despite that the optimal objective value of OPT is unknown.

To proceed, we need the following notation. For a given power assignment (y_l, p_l) to OPT (i.e., satisfying constraints (1), (2), (9)), define $\bar{\mathbf{x}} = (\bar{r}(f), \bar{r}_l(f), y_l, p_l)$ as a feasible solution to OPT, where $(\bar{r}(f), \bar{r}_l(f))$ is the optimal solution to the following linear program (LP).

$$\textbf{OPT}(y_l, p_l)\textbf{:} \quad \max \sum_{f\in\mathcal{F}} w(f)r(f)$$
$$\text{s.t.} \sum_{l\in\mathcal{L}_i^{\text{Out}}} r_l(f) = r(f) \qquad (f \in \mathcal{F}, i \in \mathcal{N}, i = s(f))$$
$$\sum_{l\in\mathcal{L}_i^{\text{Out}}}^{l\neq(i,s(f))} r_l(f) = \sum_{l\in\mathcal{L}_i^{\text{In}}}^{l\neq(d(f),i)} r_l(f) \qquad (f \in \mathcal{F}, i \in \mathcal{N}, i \neq s(f), d(f))$$
$$\sum_{f\in\mathcal{F}} r_l(f) \leq \bar{c}_l \qquad (l \in \mathcal{L}) \ ,$$

where $\bar{c}_l = B_l \log_2(1 + \frac{p_l \cdot h_l}{\eta B_l})$. Note that $\text{OPT}(y_l, p_l)$ is an LP once we set the power variables in OPT to values (y_l, p_l).

For a feasible solution $\bar{\mathbf{x}} = (\bar{r}(f), \bar{r}_l(f), y_l, p_l)$ to OPT, we define a feasible solution $\mathbf{x}^\dagger = (r^\dagger(f), r_l^\dagger(f), y_l, p_l)$ to OPT-R as follows. In $\mathbf{x}^\dagger = (r^\dagger(f), r_l^\dagger(f), y_l, p_l)$, we let $(r^\dagger(f), r_l^\dagger(f))$ be the optimal flow routing solution to OPT-R with given (y_l, p_l). That is, $(r^\dagger(f), r_l^\dagger(f))$ is the optimal solution to the following LP, in which the power variables in OPT-R are set to given values (y_l, p_l).

$$\textbf{OPT-R}(y_l, p_l)\textbf{:} \quad \max \sum_{f \in \mathcal{F}} w(f) r(f)$$

$$\text{s.t.} \sum_{l \in \mathcal{L}_i^{\text{Out}}} r_l(f) = r(f) \qquad (f \in \mathcal{F}, i \in \mathcal{N}, i = s(f))$$

$$\sum_{l \in \mathcal{L}_i^{\text{Out}}}^{l \neq (i, s(f))} r_l(f) = \sum_{l \in \mathcal{L}_i^{\text{In}}}^{l \neq (d(f), i)} r_l(f) \qquad (f \in \mathcal{F}, i \in \mathcal{N}, i \neq s(f), d(f))$$

$$\sum_{f \in \mathcal{F}} r_l(f) \leq c_l^\dagger \qquad (l \in \mathcal{L}) \; ,$$

where $c_l^\dagger$ is a linear approximation of link l's capacity under transmission power p_l.

Remark 1 *Recall that we use constraints (16) to replace constraints (8) in OPT-R. When link l's power is fixed at p_l, we can determine which line segment is involved in our linear approximation of $\ln(1 + s_l)$. Suppose the k-th linear segment is used, i.e., $s_l^{(k-1)} \leq \frac{p_l \cdot h_l}{\eta B_l} \leq s_l^{(k)}$. Then, link l's approximated capacity can be written as $c_l^\dagger = \frac{B_l}{\ln 2} \cdot g_l^{(k)}(\frac{p_l \cdot h_l}{\eta B_l})$.* $\square$

To quantify the performance gap between our solution to OPT-R and the optimal solution to OPT, we will first show that for any feasible power assignment (p_l, y_l), the objective value gap between $\bar{\mathbf{x}}$ and $\mathbf{x}^\dagger$ is at most $\epsilon \cdot \sum_{f \in \mathcal{F}} \sum_{l \in \mathcal{L}_{s(f)}^{\text{Out}}} \frac{B_l}{\ln 2} w(f)$. Then, we will show that the gap between the optimal objective values of OPT and OPT-R is also bounded by $\epsilon \cdot \sum_{f \in \mathcal{F}} \sum_{l \in \mathcal{L}_{s(f)}^{\text{Out}}} \frac{B_l}{\ln 2} w(f)$.

Lemma 4 *For given (y_l, p_l), denote $\bar{z}$ and $z^\dagger$ the objective values of solution $\bar{\mathbf{x}}$ (to OPT) and solution $\mathbf{x}^\dagger$ (to OPT-R), respectively. Then we have $\bar{z} - z^\dagger \leq \epsilon \cdot \sum_{f \in \mathcal{F}} \sum_{l \in \mathcal{L}_{s(f)}^{\text{Out}}} \frac{B_l}{\ln 2} w(f)$.*

We find that it is not easy to characterize the gap between $\bar{z}$ and $z^\dagger$ directly. Since $\bar{z}$ is the optimal value of OPT(y_l, p_l) and $z^\dagger$ is the optimal objective value of OPT-R(y_l, p_l), we study the dual problems of OPT(y_l, p_l) and OPT-R(y_l, p_l) and quantify $\bar{z} - z^\dagger$ in the dual domain.

Proof Note that $\bar{z}$ is the optimal objective value of OPT(y_l, p_l) and $z^\dagger$ is the optimal objective value of OPT-R(y_l, p_l). Consider the dual problems of OPT(y_l, p_l) and OPT-R(y_l, p_l). Denote D(y_l, p_l) and D-R(y_l, p_l) as the dual problems of OPT(y_l, p_l) and OPT-R(y_l, p_l), respectively. Note that D(y_l, p_l) and D-R(y_l, p_l) will have the same constraints, but different objective functions.

Denote the dual variables corresponding to the first group of constraints in OPT(y_l, p_l) and OPT-R(y_l, p_l) as $u(f), f \in \mathcal{F}$. Denote the dual variables corresponding to the second group of constraints in OPT(y_l, p_l) and OPT-R(y_l, p_l) as $v_i(f), f \in \mathcal{F}, i \in \mathcal{N}, i \neq s(f), d(f)$. Denote the dual variables corresponding to the third group of constraints in OPT(y_l, p_l) and OPT-R(y_l, p_l) as $q_l, l \in \mathcal{L}$. Then, D(y_l, p_l) can be written as

$$\text{D}(y_l, p_l): \quad \min \sum_{l \in \mathcal{L}} \bar{c}_l q_l$$

$$\text{s.t.} - u(f) \geq w(f) \ (f \in \mathcal{F}) \tag{17}$$

$$v_i(f) + q_l \geq 0 \ (f \in \mathcal{F}, l \in \mathcal{L}^{\text{Out}}(i), i \neq s(f), d(f))$$

$$- v_i(f) + q_l \geq 0 \ (f \in \mathcal{F}, l \in \mathcal{L}^{\text{In}}(i), i \neq s(f), d(f))$$

$$u(f) + q_l \geq 0 \ (f \in \mathcal{F}, l \in \mathcal{L}^{\text{Out}}(s(f))) \tag{18}$$

$$u(f), v_i(f) \text{ unrestricted}, q_l \geq 0.$$

Dual problem D-R(y_l, p_l) can be written as

$$\text{D-R}(y_l, p_l): \quad \min \sum_{l \in \mathcal{L}} c_l^\dagger q_l$$

$$\text{s.t.} \quad \text{All constraints in D}(y_l, p_l).$$

Combining (17) and (18) gives us $q_l \geq w(f), l \in \mathcal{L}^{\text{Out}}(s(f)), f \in \mathcal{F}$. Since these two dual problems are both minimization problems, it is easy to see that the solution with $q_l^* = w(f), (l \in \mathcal{L}^{\text{Out}}(s(f)), f \in \mathcal{F})$ and all the other variables equal to zero is the optimal solution to both D(y_l, p_l) and D-R(y_l, p_l). That is

$$q_l^* = \begin{cases} w(f) & \text{if link } l \text{ is an outgoing link from } s(f); \\ 0 & \text{otherwise.} \end{cases} \tag{19}$$

Then, we have

$$\bar{z} - z^{\dagger} = \sum_{l \in \mathcal{L}} \bar{c}_l q_l^* - \sum_{l \in \mathcal{L}} c_l^{\dagger} q_l^* = \sum_{l \in \mathcal{L}} (\bar{c}_l - c_l^{\dagger}) q_l^* = \sum_{f \in \mathcal{F}} \sum_{l \in \mathcal{L}^{\mathrm{Out}}(s(f))} (\bar{c}_l - c_l^{\dagger}) w(f) \ , \tag{20}$$

where the first equality holds due to the strong duality property [1, Chapter 6] and the third equality holds due to (19). Note that the gap between $\bar{c}_l$ and $c_l^{\dagger}$ is

$$\bar{c}_l - c_l^{\dagger} \leq \frac{B_l}{\ln 2} \epsilon, \tag{21}$$

since the maximum error of our linear approximation is ϵ. Combining (20) and (21) gives us

$$\bar{z} - z^{\dagger} \leq \epsilon \cdot \sum_{f \in \mathcal{F}} \sum_{l \in \mathcal{L}^{\mathrm{Out}}(s(f))} \frac{B_l}{\ln 2} w(f) \ .$$

This completes the proof. □

Now we are ready to characterize the performance gap between the optimal objective values of OPT-R and OPT as follows.

Theorem 1 *The gap between the optimal objective values of OPT and OPT-R is no more than* $\epsilon \cdot \sum_{f \in \mathcal{F}} \sum_{l \in \mathcal{L}_{s(f)}^{\mathrm{Out}}} \frac{B_l}{\ln 2} w(f)$.

Proof Denote $\mathbf{x}^*$ and z^* the optimal solution and the optimal objective value of OPT, respectively. From Lemma 4, since $\mathbf{x}^*$ is a particular case of $\bar{\mathbf{x}}$, we know that there exists a feasible solution of OPT-R $\mathbf{x}_R$ corresponding to $\mathbf{x}^*$ such that the performance gap between $\mathbf{x}^*$ and $\mathbf{x}_R$ is at most $\epsilon \cdot \sum_{f \in \mathcal{F}} \sum_{l \in \mathcal{L}_{s(f)}^{\mathrm{Out}}} \frac{B_l}{\ln 2} w(f)$. Denote z_R the objective value of solution $\mathbf{x}_R$ to OPT-R. Then, we have

$$z^* - z_R \leq \epsilon \cdot \sum_{f \in \mathcal{F}} \sum_{l \in \mathcal{L}_{s(f)}^{\mathrm{Out}}} \frac{B_l}{\ln 2} w(f). \tag{22}$$

Denote z_R^* the optimal objective value of OPT-R. Since z_R is the objective value of a feasible solution to OPT-R while z_R^* is the optimal objective value of OPT-R, we have

$$z_R^* \geq z_R. \tag{23}$$

Combining (22) and (23), we have $z^* - z_R^* \leq \epsilon \cdot \sum_{f \in \mathcal{F}} \sum_{l \in \mathcal{L}_{s(f)}^{\mathrm{Out}}} \frac{B_l}{\ln 2} w(f)$.

Based on Theorem 1, we are able to give an algorithm to obtain a near-optimal solution to OPT with performance guarantee as follows.

Algorithm 2 Input: *Given a desired performance gap γ for the solution.*

1. *Compute ϵ based on*
$$\epsilon \cdot \sum_{f \in \mathcal{F}} \sum_{l \in \mathcal{L}^{\text{Out}}_{s(f)}} \frac{B_l}{\ln 2} w(f) = \gamma. \tag{24}$$
2. *Compute $m_l^{(k)}$ and $s_l^{(k)}$ by Algorithm 1.*
3. *Construct OPT-R based on $m_l^{(k)}$ and $s_l^{(k)}$.*
4. *Solve OPT-R optimally with CPLEX.*

Upon the completion of Algorithm 2, we will have a near-optimal solution to OPT with a guaranteed performance bound (no more than γ from the optimal objective value).

4 Maximizing Throughput and Minimizing Network-wide Energy Consumption

In the previous section, we have shown how to maximize network throughput while satisfying a given total network-wide energy budget. The problem was formulated as a *single objective* optimization problem OPT. In this section, we take one step further. We are interested in maximizing network throughput while minimizing energy consumption. We cast this problem into a *multicriteria* optimization problem with two objectives. Mathematically, this problem can be written as follows:

$$\begin{aligned}
\textbf{MP:} \quad & \max && \sum_{f \in \mathcal{F}} w(f) r(f) \\
& \min && \sum_{l \in \mathcal{L}} (p_l + y_l P_d) \\
& \text{s.t.} && \text{Constraints } (1), (2), (3), (4), (8) \\
& && \text{Variables } y_l \in \{0, 1\}, p_l, r_l(f), r(f) \geq 0 \ (l \in \mathcal{L}, f \in \mathcal{F}).
\end{aligned}$$

As we can see, minimizing network-wide energy consumption and maximizing network throughput are two conflicting objectives. For such a problem, it is in general not possible to find a single feasible solution that is optimal for both objectives at the same time. For example, when P is minimized (i.e., 0), U is also 0 but is not maximized. Therefore, it is important to clarify what we mean by optimal solutions.

In this paper, we are interested in finding the so-called weakly Pareto-optimal solutions [5]. Weakly Pareto-optimal solutions are optimal in the sense that it is impossible to improve the performance of both objectives simultaneously. Specifically, we say that (P^*, U^*) is a weakly Pareto-optimal point to problem MP if there does not exist another solution to problem MP with (P, U) such that $P < P^*$ and $U > U^*$.

To find weakly Pareto-optimal points, we transform the multicriteria optimization problem into a single objective optimization problem. This can be done by moving the second objective (i.e., $\sum_{l\in\mathcal{L}}(p_l + y_l P_d)$) into the constraints as follows.

$$
\begin{aligned}
\textbf{SP}(P_{\text{net}})\textbf{:} \quad \text{max} \quad & \sum_{f\in\mathcal{F}} w(f)r(f) \\
\text{s.t.} \quad & \sum_{l\in\mathcal{L}} (p_l + y_l P_d) \le P_{\text{net}} \\
& \text{Constraints}(1), (2), (3), (4), (8) \\
& \text{Variables } y_l \in \{0, 1\}, p_l, r_l(f), r(f) \ge 0 \ (l \in \mathcal{L}, f \in \mathcal{F}).
\end{aligned}
$$

We see that this single objective optimization problem is precisely the same as OPT that we studied earlier. For a fixed value of P_{net}, solving SP(P_{net}) will give us *one* weakly Pareto-optimal point of problem MP [5]. By varying P_{net} from 0 to $P_{\text{net}}^{\max} = |\mathcal{L}| \cdot (P_{\max} + P_d)$, we can obtain all the weakly Pareto-optimal points. These points provide a mapping from the network-wide energy budget P_{net} to the maximum network throughput U, which we denote as $\pi : P_{\text{net}} \to U$. This mapping $U = \pi(P_{\text{net}})$ is an optimal throughput-energy curve, which characterizes how the maximum network throughput changes as the total network-wide energy consumption rate varies. This curve is useful for network operators to have a holistic view of the entire optimal trade-off curve and decide which point to choose so as to meet their needs.

We have several interesting properties about this optimal throughput-energy curve $U = \pi(P_{\text{net}})$, which are shown in Property 1.

Property 1 *The optimal throughput-energy curve $U = \pi(P_{\text{net}})$ has the following properties.*

1. *$\pi(P_{\text{net}})$ is a nondecreasing function of P_{net}.*

2. *$\pi(P_{\text{net}})$ has a starting point $(P_{\text{start}}, 0)$, i.e., $\pi(P_{\text{net}}) = 0$ for $P_{\text{net}} \le P_{\text{start}}$ and $\pi(P_{\text{net}}) > 0$ for $P_{\text{net}} > P_{\text{start}}$.*

3. *$\pi(P_{\text{net}})$ has a saturation point $(P_{\text{sat}}, U_{\text{sat}})$, i.e., $\pi(P_{\text{net}}) = U_{\text{sat}}$ for $P_{\text{net}} \ge P_{\text{sat}}$ and $\pi(P_{\text{net}}) < U_{\text{sat}}$ for $P_{\text{net}} < P_{\text{sat}}$.*

Proof We prove each property as follows.

1. Assume $P_{\text{net}}^{(1)} < P_{\text{net}}^{(2)}$. We need to show that $U(P_{\text{net}}^{(1)}) \le U(P_{\text{net}}^{(2)})$. Note that $U(P_{\text{net}}^{(1)})$ and $U(P_{\text{net}}^{(2)})$ are the optimal objectives of SP$(P_{\text{net}}^{(1)})$ and SP$(P_{\text{net}}^{(2)})$, respectively. Since $P_{\text{net}}^{(1)} < P_{\text{net}}^{(2)}$, the feasible region of SP$(P_{\text{net}}^{(1)})$ falls inside the feasible region of SP$(P_{\text{net}}^{(2)})$. Thus, we have $U(P_{\text{net}}^{(1)}) \le (P_{\text{net}}^{(2)})$.

2. Such starting point exists because when a link is active, it must consume a constant power P_d. For a session to have positive throughput, it must activate all the links along the path that are used by this session for transporting data. Thus, P_{start} can be determined by the session that uses the minimum number of hops from its source to its destination. Denote m_f the minimum hops of session f. Then, P_{start} can be written as $P_{\text{start}} = P_d \cdot \min\{m_f : f \in \mathcal{F}\}$.

3. The saturation point $(P_{\text{sat}}, U_{\text{sat}})$ can be determined as follows. We can first compute the maximum network throughput without network-wide energy constraint, i.e., solving the following optimization problem.

$$\begin{aligned} \max \quad & \sum_{f \in \mathcal{F}} w(f) r(f) \\ \text{s.t.} \quad & \text{Constraints } (1), (2), (3), (4), (8). \end{aligned}$$

   The optimal objective value of the above problem is U_{sat}. Then, we determine the minimum

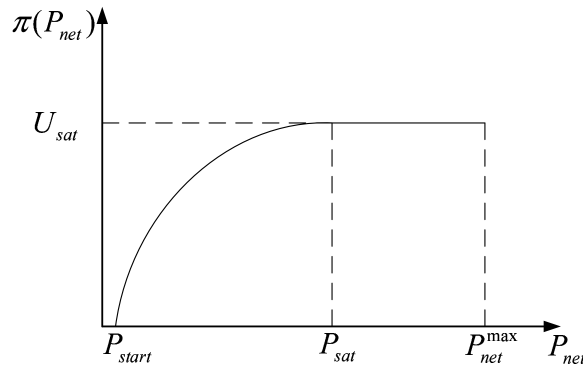

Figure 4: An illustration of optimal throughput-energy curve.

energy that can achieves this throughput by solving the following optimization problem.

$$\begin{aligned} \text{min} \quad & \sum_{l \in \mathcal{L}} (p_l + y_l P_c) \\ \text{s.t.} \quad & w(f) r(f) = U_{\text{sat}} \\ & \text{Constraints } (1), (2), (3), (4), (8). \end{aligned}$$

Based on Property 1, Fig. 4 illustrates a typical optimal throughput-energy curve for a multi-hop wireless network.

5 Numerical Results

In this section, we present some numerical results to illustrate our theoretical findings in Section 3 and 4.

5.1 Simulation Settings

We consider a 50-node network deployed in a 1000×1000 square area and a 100-node network deployed in a 1500×1500 square area. The topologies of the 50-node network and 100-node network are shown in Fig. 5 and Fig. 6, respectively. We assume that all units are normalized with appropriate dimensions. We assume the maximum transmission range is 200 and the maximum transmission power is $P_{\max} = 2$. We assume node device power consumption is $P_d = 0.2$. The

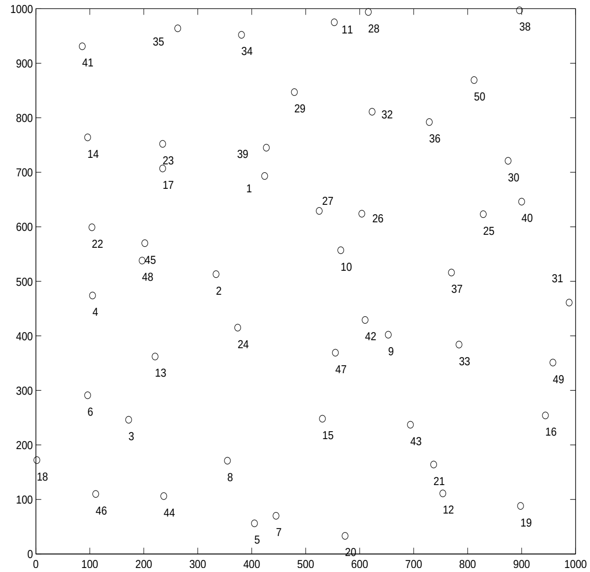

Figure 5: The topology for a 50-node network.

Table 2: Each session's source node, destination node, and weight for the 50-node network.

Session f	Source node $s(f)$	Dest. node $d(f)$	Weight $w(f)$
1	10	35	0.5
2	35	21	0.9
3	5	23	0.7
4	43	14	0.6
5	29	7	0.8

channel bandwidth is $B_l = 1$ for all links and channel gain is $h_l = d_l^{-4}$, where d_l is the distance between link l's transmitting node and receiving node.

5.2 Results for the 50-node Network

Within this network, we assume there are $|\mathcal{F}| = 5$ user sessions, with source node and destination node of each session chosen randomly. Table 2 lists the source node, destination node, and weight for each session in the network.

5.2.1 Near-Optimal Solution for OPT

In this case study, we assume the maximum network-wide energy consumption rate $P_{\text{net}} = 40$. We set the maximum acceptable performance gap between the optimal objectives of OPT and

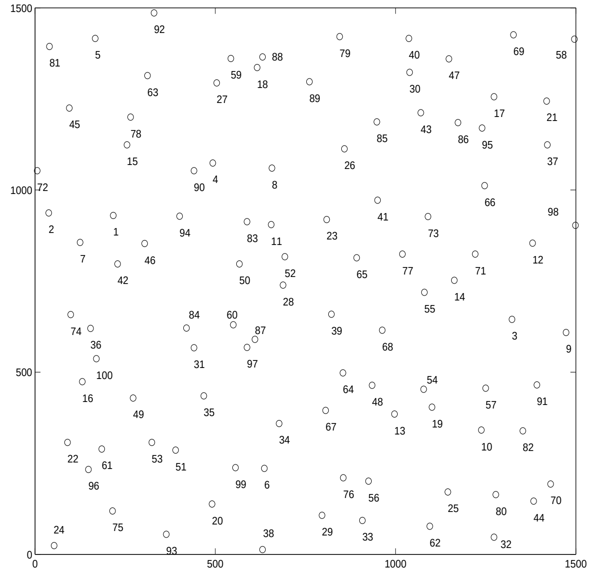

Figure 6: The topology for a 100-node network.

linear approximation OPT-R as $\gamma = 0.1$. We apply Algorithm 2 here. Based on (24), we compute $\epsilon = \frac{\gamma \cdot \ln 2}{\sum_{f \in \mathcal{F}} \sum_{l \in \mathcal{L}^{\mathrm{Out}}_{s(f)}} \frac{B_l}{\ln 2} w(f)} = 0.0046$. Based on ϵ, we compute the piece-wise linear approximation according to Algorithm 1.

Then we can use CPLEX to solve OPT-R. We obtain that the maximum network throughput is $U = 22.12$. The achieved session data rates are $r_1 = 4.41$, $r_2 = 6.39$, $r_3 = 9.37$, $r_4 = 3.89$, and $r_5 = 6.62$. Our algorithm gives power control and flow routing solutions for the network. We list the power assignment for each active link in Table 3, and the flow routing results in Table 4.

5.2.2 The Optimal Throughput-Energy Curve

For the same 50-node network instance, we characterize its optimal throughput-energy curve based on our theoretical results in Section 4. We show the optimal throughput-energy curve in Fig. 7. From the figure, we can see all three properties as stated in Property 1. As shown in the figure, the curve is nondecreasing. The network throughput keeps at zero when the network energy consumption rate is no greater than P_{start}. For the starting point $(P_{\mathrm{start}}, 0)$, since session 1 needs at least 5 hops , we have $P_{\mathrm{start}} = 5 \cdot P_d = 1$. For the saturation point $(P_{\mathrm{sat}}, U_{\mathrm{sat}})$, we get $(P_{\mathrm{sat}}, U_{\mathrm{sat}}) = (106.20, 36.14)$. The network throughput stops increasing and keeps as 36.14 when

Table 3: Power assignment on each active link in the final solution for the 50-node network.

Link	Power	Link	Power	Link	Power
$1 \to 27$	0.1819	$1 \to 23$	0.4317	$1 \to 17$	0.4658
$2 \to 45$	0.1958	$2 \to 24$	0.0370	$3 \to 44$	0.2050
$3 \to 13$	0.1805	$3 \to 6$	0.0350	$4 \to 45$	0.2083
$4 \to 22$	0.1692	$4 \to 13$	0.2441	$5 \to 44$	0.2652
$5 \to 8$	0.1775	$5 \to 7$	0.0313	$6 \to 4$	0.6487
$7 \to 15$	0.4290	$7 \to 8$	0.1534	$8 \to 44$	0.0707
$8 \to 15$	0.2924	$8 \to 7$	0.1209	$8 \to 3$	0.5524
$9 \to 43$	0.1794	$9 \to 10$	0.2835	$10 \to 47$	0.5756
$10 \to 42$	0.0952	$10 \to 27$	0.3033	$10 \to 26$	0.0101
$10 \to 9$	0.2166	$10 \to 1$	0.2355	$11 \to 34$	0.2547
$11 \to 32$	0.1617	$13 \to 4$	0.4853	$13 \to 3$	0.0908
$14 \to 22$	0.2196	$15 \to 47$	0.2544	$15 \to 8$	0.4918
$15 \to 7$	0.5515	$17 \to 45$	0.1424	$17 \to 23$	0.0151
$17 \to 14$	0.1431	$22 \to 45$	0.0628	$22 \to 17$	0.3000
$22 \to 14$	0.2092	$24 \to 47$	0.3587	$24 \to 2$	0.0575
$25 \to 37$	0.1283	$26 \to 32$	0.3506	$27 \to 39$	0.4733
$27 \to 10$	0.3033	$27 \to 1$	0.1177	$29 \to 39$	0.5181
$29 \to 34$	0.1950	$29 \to 32$	0.0776	$29 \to 1$	0.6365
$30 \to 25$	0.0791	$32 \to 36$	0.0774	$32 \to 11$	0.2840
$33 \to 43$	0.5081	$34 \to 35$	0.4009	$34 \to 29$	0.3055
$34 \to 11$	0.1450	$35 \to 41$	0.3099	$35 \to 34$	0.4009
$36 \to 30$	0.3999	$37 \to 33$	0.1787	$39 \to 29$	0.0787
$39 \to 27$	0.3061	$39 \to 23$	0.1054	$39 \to 17$	0.5299
$41 \to 14$	0.2310	$42 \to 15$	0.4273	$42 \to 10$	0.2433
$43 \to 47$	0.3793	$43 \to 21$	0.4274	$43 \to 9$	0.2347
$44 \to 5$	0.3408	$44 \to 3$	0.6235	$45 \to 23$	0.1872
$45 \to 22$	0.0306	$45 \to 17$	0.2270	$45 \to 4$	0.1253
$45 \to 2$	0.1260	$47 \to 43$	0.3982	$47 \to 42$	0.0315
$47 \to 24$	0.5573	$47 \to 15$	0.1061		

Table 4: Flow routing results for the 50-node network.

Session f	Flow rate on each link attributed to session f
1	$r_{10\to27}(1) = 2.48$, $r_{10\to26}(1) = 1.93$, $r_{11\to34}(1) = 1.93$ $r_{26\to32}(1) = 1.93$, $r_{27\to39}(1) = 2.48$, $r_{29\to34}(1) = 2.48$ $r_{32\to11}(1) = 1.93$, $r_{34\to35}(1) = 4.41$, $r_{39\to29}(1) = 2.48$
2	$r_{1\to27}(2) = 1.65$, $r_{2\to24}(2) = 1.98$, $r_{9\to43}(2) = 1.65$ $r_{10\to9}(2) = 1.65$, $r_{11\to32}(2) = 1.38$, $r_{14\to22}(2) = 1.98$ $r_{22\to45}(2) = 1.98$, $r_{24\to47}(2) = 1.98$, $r_{25\to37}(2) = 2.76$ $r_{27\to10}(2) = 1.65$, $r_{29\to32}(2) = 1.38$,$r_{29\to1}(2) = 1.65$, $r_{30\to25}(2) = 2.76$, $r_{32\to36}(2) = 2.76$, $r_{33\to43}(2) = 2.76$ $r_{34\to29}(2) = 3.03$, $r_{34\to11}(2) = 1.38$, $r_{35\to41}(2) = 1.98$ $r_{35\to34}(2) = 4.41$, $r_{36\to30}(2) = 2.76$, $r_{37\to33}(2) = 2.76$ $r_{41\to14}(2) = 1.98$, $r_{43\to21}(2) = 6.39$, $r_{45\to2}(2) = 1.98$ $r_{47\to43}(2) = 1.98$
3	$r_{1\to23}(3) = 1.93$, $r_{1\to17}(3) = 0.28$, $r_{2\to45}(3) = 0.55$ $r_{3\to13}(3) = 3.03$, $r_{3\to6}(3) = 2.76$, $r_{4\to45}(3) = 2.80$ $r_{4\to22}(3) = 2.98$, $r_{5\to44}(3) = 1.93$, $r_{5\to8}(3) = 3.03$ $r_{5\to7}(3) = 4.41$, $r_{6\to4}(3) = 2.76$, $r_{7\to15}(3) = 1.93$ $r_{7\to8}(3) = 2.48$, $r_{8\to44}(3) = 1.65$, $r_{8\to15}(3) = 1.65$ $r_{8\to3}(3) = 2.21$, $r_{10\to27}(3) = 1.65$, $r_{10\to1}(3) = 1.38$ $r_{13\to4}(3) = 3.03$, $r_{15\to47}(3) = 3.58$, $r_{17\to23}(3) = 5.24$ $r_{22\to45}(3) = 0.78$, $r_{22\to17}(3) = 2.21$, $r_{24\to2}(3) = 0.55$ $r_{27\to39}(3) = 0.83$, $r_{27\to1}(3) = 0.83$, $r_{39\to23}(3) = 0.83$ $r_{42\to10}(3) = 3.03$, $r_{44\to3}(3) = 3.58$, $r_{45\to23}(3) = 1.38$ $r_{45\to17}(3) = 2.76$, $r_{47\to42}(3) = 3.03$, $r_{47\to24}(3) = 0.55$
4	$r_{1\to17}(4) = 1.93$, $r_{2\to45}(4) = 1.93$, $r_{9\to10}(4) = 1.93$ $r_{10\to27}(4) = 1.93$, $r_{17\to14}(4) = 1.93$, $r_{22\to14}(4) = 1.93$ $r_{24\to2}(4) = 1.93$, $r_{27\to1}(4) = 1.93$, $r_{43\to47}(4) = 1.93$ $r_{43\to9}(4) = 1.93$, $r_{45\to22}(4) = 1.93$, $r_{47\to24}(4) = 1.93$
5	$r_{1\to27}(5) = 1.65$, $r_{3\to44}(5) = 2.21$, $r_{4\to13}(5) = 2.21$ $r_{5\to7}(5) = 2.21$, $r_{8\to7}(5) = 2.21$, $r_{10\to47}(5) = 2.48$ $r_{10\to42}(5) = 1.93$, $r_{13\to3}(5) = 2.21$, $r_{15\to8}(5) = 2.21$ $r_{15\to7}(5) = 2.21$, $r_{17\to45}(5) = 2.21$, $r_{27\to10}(5) = 4.41$ $r_{29\to39}(5) = 4.96$, $r_{29\to1}(5) = 1.65$, $r_{39\to27}(5) = 2.76$ $r_{39\to17}(5) = 2.21$, $r_{42\to15}(5) = 1.93$, $r_{44\to5}(5) = 2.21$ $r_{45\to4}(5) = 2.21$, $r_{47\to15}(5) = 2.48$

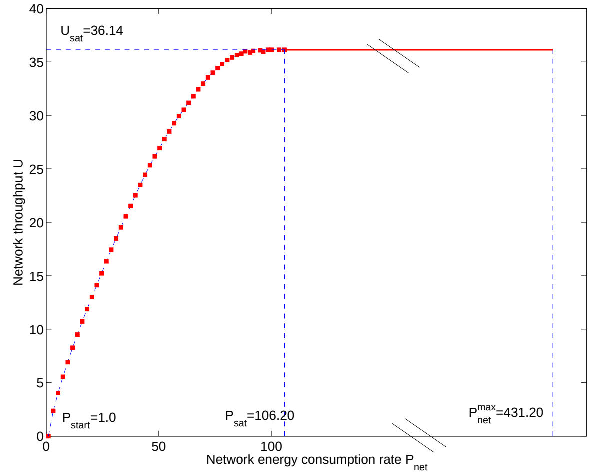

Figure 7: The optimal throughput-energy curve for the 50-node network, where the "\\" sign in the figure indicates nonlinear scale for $P_{\rm net} \in [106.20, 431.20]$.

the network energy consumption rate exceeds $P_{\rm sat} = 106.20$.

5.3 Results for the 100-node Network

For the 100-node network, we assume that there are $|\mathcal{F}| = 10$ active sessions in the network, with each session's source node, destination node, and weight given in Table 5.

We assume that maximum network-wide energy consumption rate $P_{\rm net} = 100$. By employing our method, we obtain that the maximum network throughput is $U = 42.00$. The achieved session data rates are $r_1 = 10.86$, $r_2 = 1.63$, $r_3 = 7.09$, $r_4 = 4.03$, $r_5 = 9.71$, $r_6 = 4.00$, $r_7 = 9.90$, $r_8 = 4.91$, and $r_9 = 8.08$, and $r_{10} = 7.19$. The detailed results for power assignment and flow routing are given in Table 6 Table 7. The optimal throughput-energy curve for the 100-node network is shown in Fig. 8.

6 Conclusion

Network-wide energy consumption has become an important concern for network operators. In this paper, we studied two tightly coupled problems for network-wide energy conservation. In the first problem, we studied how to maximize network throughput under a network-wide energy constraint. We formulated this problem into a mixed-integer nonlinear program (MINLP) and

Table 5: Each session's source node, destination node, and weight for the 100-node network.

Session f	Source node $s(f)$	Dest. node $d(f)$	Weight $w(f)$
1	40	26	0.9
2	27	17	0.8
3	4	55	0.7
4	31	41	0.6
5	78	100	0.8
6	7	83	0.6
7	73	91	0.3
8	12	10	0.4
9	64	38	0.6
10	51	56	0.5

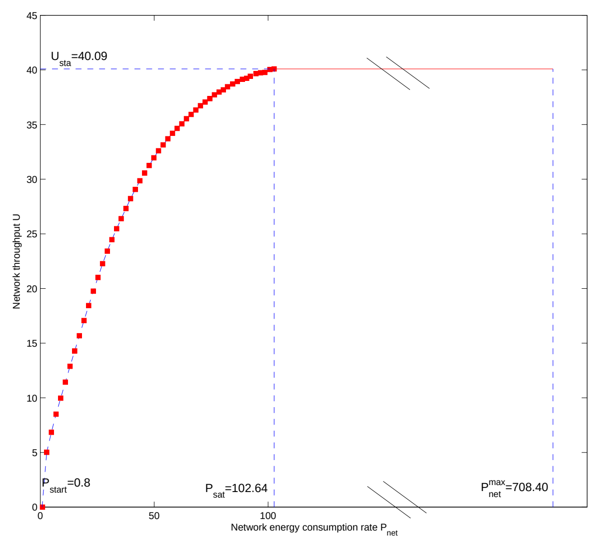

Figure 8: The optimal throughput-energy curve for the 100-node network, where the "\\" sign in the figure indicates nonlinear scale for $P_{\text{net}} \in [102.64, 708.40]$.

proposed a near-optimal solution with guaranteed performance bound. In the second problem, we explored joint optimization of both network throughput and energy consumption via a multicriteria optimization framework. We showed that the weakly Pareto-optimal points in the solution can characterize an optimal throughput-energy curve. The results in this paper offer both solutions and insights to network operators when total energy consumption for the entire network is of greater concern than local energy consumption.

References

[1] M.S. Bazaraa, J.J. Jarvis, and H.D. Sherali, *Linear Programming and Network Flows, 3rd edition*, John Wiley & Sons Inc., Hoboken, New Jersey, 2005.

[2] L. Chen, S.H. Low, M. Chiang, and J.C. Doyle, "Cross-layer congestion control, routing and scheduling design in ad hoc wireless networks," in *Proc. IEEE INFOCOM*, 13 pages, Barcelona, Spain, April 2006.

[3] IBM ILOG CPLEX Optimizer, http://www-01.ibm.com/software/integration/optimization/cplex-optimizer/.

[4] S. Cui, A.J. Goldsmith, and A. Bahai, "Energy-constrained modulation optimization," *IEEE Trans. on Wireless Communications*, vol. 4, no. 5, pp. 2349–2360, Sep. 2005.

[5] M. Ehrgott, *Multicriteria Optimization, Second Edition*, Springer-Verlag, New York, 2010.

[6] R. Fletcher and S. Leyffer, "Solving mixed integer programs by outer approximation," *Mathematical Programming*, vol. 66, no. 1–3, pp. 327–349, 1994.

[7] O.K. Gupta and A. Ravindran, "Branch and bound experiments in convex nonlinear integer programming," *Management Science*, vol. 31, no. 12, pp. 1533–1546, 1985.

[8] S. Huang, X. Liu, and Z. Ding, "Distributed power control for cognitive user access based on primary link control feedback," in *Proc. IEEE INFOCOM*, pp. 1280–1288, San Diego, CA, March 14–19, 2010.

[9] M.R. Garey and D.S. Johnson, *Computers and Intractability: A Guide to the Theory of NP-completeness*, W.H. Freeman and Company, pp. 245–248, New York, NY, 1979.

[10] A.M. Geoffrion, "A generalized Benders' decomposition," *Journal of optimization theory and applications*, vol. 10, no. 4, pp. 237–260, 1972.

[11] C. Jiang, Y. Shi, Y.T. Hou, and S. Kompella, "On optimal throughput-energy curve for multi-hop wireless networks," in *Proc. IEEE INFOCOM*, pp. 1341–1349, Shanghai, China, April 10–15, 2011.

Table 6: Power assignment on each active link in the final solution for the 100-node network.

Link	Power	Link	Power	Link	Power
$1 \rightarrow 46$	0.1610	$34 \rightarrow 67$	1.5375	$65 \rightarrow 41$	0.3069
$1 \rightarrow 42$	0.2142	$34 \rightarrow 6$	0.4389	$65 \rightarrow 39$	1.0259
$2 \rightarrow 7$	0.2847	$35 \rightarrow 84$	0.2735	$66 \rightarrow 73$	0.5698
$3 \rightarrow 91$	0.3482	$36 \rightarrow 100$	0.3999	$66o71$	0.2038
$3 \rightarrow 9$	0.1693	$39 \rightarrow 68$	0.6296	$67 \rightarrow 76$	1.3448
$4 \rightarrow 83$	0.9835	$39 \rightarrow 64$	0.9111	$67 \rightarrow 48$	0.0920
$4 \rightarrow 8$	1.0165	$40 \rightarrow 47$	1.0196	$67 \rightarrow 34$	0.4997
$6 \rightarrow 99$	0.0637	$40 \rightarrow 30$	0.9804	$67 \rightarrow 13$	0.0635
$6 \rightarrow 34$	0.3062	$41 \rightarrow 77$	0.2932	$68 \rightarrow 64$	0.2041
$7 \rightarrow 74$	1.7122	$41 \rightarrow 26$	1.2846	$68 \rightarrow 54$	1.0492
$7 \rightarrow 46$	0.1229	$41 \rightarrow 23$	0.1969	$68 \rightarrow 48$	0.7467
$7 \rightarrow 1$	0.1649	$42 \rightarrow 74$	1.0565	$71 \rightarrow 55$	0.6433
$8 \rightarrow 83$	0.1445	$42 \rightarrow 36$	0.9435	$71 \rightarrow 14$	0.2603
$8 \rightarrow 11$	0.2208	$43 \rightarrow 86$	0.0492	$72 \rightarrow 2$	0.2990
$9 \rightarrow 91$	0.2227	$43 \rightarrow 85$	0.3158	$73 \rightarrow 77$	0.5455
$10 \rightarrow 80$	0.3385	$45 \rightarrow 72$	2.0000	$73 \rightarrow 71$	0.2047
$10 \rightarrow 25$	0.4205	$46 \rightarrow 94$	0.3406	$73 \rightarrow 41$	0.8028
$11 \rightarrow 52$	0.0571	$46 \rightarrow 42$	0.0634	$73 \rightarrow 14$	0.4035
$11 \rightarrow 23$	0.9333	$47 \rightarrow 86$	0.2463	$74 \rightarrow 100$	0.3717
$12 \rightarrow 71$	2.0000	$47 \rightarrow 43$	0.2360	$74 \rightarrow 36$	0.0181
$13 \rightarrow 56$	1.8806	$47 \rightarrow 17$	0.1470	$76 \rightarrow 56$	0.0249
$13 \rightarrow 54$	0.0581	$48 \rightarrow 54$	0.6765	$77 \rightarrow 65$	0.3229
$13 \rightarrow 19$	0.0613	$48 \rightarrow 19$	0.6538	$77 \rightarrow 55$	0.6875
$14 \rightarrow 77$	0.1055	$48 \rightarrow 13$	0.3289	$77 \rightarrow 41$	0.2516
$14 \rightarrow 55$	0.1035	$50 \rightarrow 52$	0.0788	$77 \rightarrow 14$	0.2097
$14 \rightarrow 3$	1.7910	$51 \rightarrow 99$	0.8556	$78 \rightarrow 45$	1.2430
$15 \rightarrow 90$	0.9260	$51 \rightarrow 35$	0.1607	$78 \rightarrow 15$	0.1874
$15 \rightarrow 1$	1.0740	$51 \rightarrow 20$	0.3715	$79 \rightarrow 40$	0.2861
$18 \rightarrow 89$	0.1069	$52 \rightarrow 65$	1.2163	$80 \rightarrow 25$	0.0982
$19 \rightarrow 57$	0.9917	$52 \rightarrow 28$	0.0143	$82 \rightarrow 91$	0.1406
$19 \rightarrow 10$	1.0083	$52 \rightarrow 23$	0.7694	$83 \rightarrow 11$	0.0557
$20 \rightarrow 99$	0.0729	$54 \rightarrow 57$	1.0144	$84 \rightarrow 87$	0.2759
$20 \rightarrow 38$	1.9271	$54 \rightarrow 19$	0.0057	$85 \rightarrow 26$	2.0000
$23 \rightarrow 65$	0.4337	$54 \rightarrow 10$	0.9799	$86 \rightarrow 95$	0.0103
$23 \rightarrow 52$	0.2177	$55 \rightarrow 68$	1.8836	$86 \rightarrow 66$	0.2518
$23 \rightarrow 41$	0.8404	$57 \rightarrow 91$	0.4561	$87 \rightarrow 28$	0.1607
$25 \rightarrow 62$	0.1981	$57 \rightarrow 82$	0.2743	$89 \rightarrow 79$	0.1058
$27 \rightarrow 18$	0.0430	$57 \rightarrow 10$	0.0381	$90 \rightarrow 94$	0.1749
$28 \rightarrow 52$	0.0117	$60 \rightarrow 50$	0.2361	$94 \rightarrow 83$	1.8668
$28 \rightarrow 39$	0.8018	$60 \rightarrow 28$	0.2986	$94 \rightarrow 46$	0.1332
$29 \rightarrow 38$	2.0000	$62 \rightarrow 33$	1.9127	$95 \rightarrow 66$	0.2907
$30 \rightarrow 85$	0.4852	$64 \rightarrow 67$	0.2590	$99 \rightarrow 34$	0.2677
$30 \rightarrow 43$	0.2821	$64 \rightarrow 48$	0.5956	$99 \rightarrow 20$	0.3143
$31 \rightarrow 60$	0.3863	$64 \rightarrow 13$	0.8886	$99 \rightarrow 6$	0.0444
$33 \rightarrow 29$	0.2502	$65 \rightarrow 77$	0.6673		

Table 7: Flow routing results for the 100-node network.

Session f	Flow rate on each link attributed to session f
1	$r_{14\to77}(1) = 1.36$, $r_{30\to85}(1) = 2.96$, $r_{30\to43}(1) = 4.09$, $r_{40\to47}(1) = 3.82$, $r_{40\to30}(1) = 7.04$, $r_{41\to26}(1) = 4.09$ $r_{43\to86}(1) = 2.27$, $r_{43\to85}(1) = 3.82$, $r_{47\to86}(1) = 1.82$, $r_{47\to43}(1) = 2.00$, $r_{66\to73}(1) = 2.72$, $r_{66\to71}(1) = 1.36$ $r_{71\to14}(1) = 1.36$, $r_{73\to41}(1) = 2.72$, $r_{77\to41}(1) = 1.36$, $r_{85\to26}(1) = 6.77$, $r_{86\to95}(1) = 2.50$, $r_{86\to66}(1) = 1.59$ $r_{95\to66}(1) = 2.50$
2	$r_{18\to89}(2) = 1.63$, $r_{27\to18}(2) = 1.63$, $r_{40\to47}(2) = 1.63$, $r_{47\to17}(2) = 1.63$, $r_{79\to40}(2) = 1.63$, $r_{89\to79}(2) = 1.63$
3	$r_{4\to83}(3) = 3.18$, $r_{4\to8}(3) = 3.89$, $r_{8\to83}(3) = 1.62$, $r_{8\to11}(3) = 2.27$, $r_{11\to52}(3) = 2.96$, $r_{11\to23}(3) = 4.11$ $r_{14\to55}(3) = 2.04$, $r_{23\to65}(3) = 3.86$, $r_{23\to41}(3) = 2.35$, $r_{41\to77}(3) = 2.35$, $r_{52\to65}(3) = 0.86$, $r_{52\to23}(3) = 2.10$ $r_{65\to77}(3) = 4.72$, $r_{77\to55}(3) = 5.03$, $r_{77\to14}(3) = 2.04$, $r_{83\to11}(3) = 4.80$
4	$r_{23\to41}(4) = 1.76$, $r_{28\to52}(4) = 2.04$, $r_{31\to60}(4) = 4.03$, $r_{50\to52}(4) = 1.99$, $r_{52\to65}(4) = 2.27$, $r_{52\to23}(4) = 1.76$ $r_{60\to50}(4) = 1.99$, $r_{60\to28}(4) = 2.04$, $r_{65\to41}(4) = 2.27$
5	$r_{1\to46}(5) = 0.05$, $r_{1\to42}(5) = 2.95$, $r_{2\to7}(5) = 3.93$, $r_{7\to74}(5) = 3.55$, $r_{7\to46}(5) = 0.38$, $r_{15\to90}(5) = 2.78$ $r_{15\to1}(5) = 3.00$, $r_{36\to100}(5) = 6.31$, $r_{42\to74}(5) = 3.18$, $r_{42\to36}(5) = 2.98$, $r_{45\to72}(5) = 3.93$, $r_{46\to42}(5) = 3.21$ $r_{72\to2}(5) = 3.93$, $r_{74\to100}(5) = 3.41$, $r_{74\to36}(5) = 3.33$, $r_{78\to45}(5) = 3.93$, $r_{78\to15}(5) = 5.78$, $r_{90\to94}(5) = 2.78$ $r_{94\to46}(5) = 2.78$
6	$r_{1\to46}(6) = 3.24$, $r_{7\to46}(6) = 0.76$, $r_{7\to1}(6) = 3.24$, $r_{46\to94}(6) = 4.00$, $r_{94\to83}(6) = 4.00$
7	$r_{3\to91}(7) = 1.82$, $r_{3\to9}(7) = 1.99$, $r_{9\to91}(7) = 1.99$, $r_{14\to3}(7) = 3.81$, $r_{19\to57}(7) = 2.95$, $r_{23\to52}(7) = 2.27$ $r_{28\to39}(7) = 2.27$, $r_{39\to68}(7) = 2.81$, $r_{39\to64}(7) = 3.19$, $r_{41\to23}(7) = 2.27$, $r_{48\to54}(7) = 3.14$, $r_{48\to19}(7) = 2.95$ $r_{52\to28}(7) = 2.27$, $r_{54\to57}(7) = 3.14$, $r_{55\to68}(7) = 0.10$, $r_{57\to91}(7) = 3.60$, $r_{57\to82}(7) = 2.50$, $r_{64\to48}(7) = 3.19$ $r_{65\to39}(7) = 3.72$, $r_{68\to48}(7) = 2.91$, $r_{71\to55}(7) = 0.10$, $r_{71\to14}(7) = 1.77$, $r_{73\to77}(7) = 4.54$, $r_{73\to71}(7) = 1.87$ $r_{73\to41}(7) = 1.45$, $r_{73\to14}(7) = 2.04$, $r_{77\to65}(7) = 3.72$, $r_{77\to41}(7) = 0.82$, $r_{82\to91}(7) = 2.50$
8	$r_{12\to71}(8) = 4.92$, $r_{13\to54}(8) = 1.02$, $r_{14\to55}(8) = 2.06$, $r_{19\to57}(8) = 1.14$, $r_{19\to10}(8) = 1.80$, $r_{48\to54}(8) = 0.94$ $r_{54\to57}(8) = 0.51$, $r_{54\to19}(8) = 2.93$, $r_{54\to10}(8) = 1.48$, $r_{55\to68}(8) = 4.92$, $r_{57\to10}(8) = 1.64$ $r_{64\to13}(8) = 1.02$, $r_{68\to64}(8) = 1.02$, $r_{68\to54}(8) = 2.95$, $r_{68\to48}(8) = 0.94$, $r_{71\to55}(8) = 2.85$, $r_{71\to14}(8) = 2.06$
9	$r_{6\to99}(9) = 4.04$, $r_{10\to80}(9) = 2.04$, $r_{10\to25}(9) = 1.99$, $r_{13\to54}(9) = 1.48$, $r_{13\to19}(9) = 2.56$, $r_{19\to10}(9) = 2.56$ $r_{20\to38}(9) = 4.04$, $r_{25\to62}(9) = 4.03$, $r_{29\to38}(9) = 4.03$, $r_{33\to29}(9) = 4.03$, $r_{34\to6}(9) = 4.04$, $r_{48\to13}(9) = 3.47$ $r_{54\to10}(9) = 1.48$, $r_{62\to33}(9) = 4.03$, $r_{64\to67}(9) = 4.04$, $r_{64\to48}(9) = 3.47$, $r_{64\to13}(9) = 0.57$, $r_{67\to34}(9) = 4.04$ $r_{80\to25}(9) = 2.04$, $r_{99\to20}(9) = 4.04$
10	$r_{6\to34}(10) = 3.56$, $r_{13\to56}(10) = 3.73$, $r_{20\to99}(10) = 2.20$, $r_{28\to39}(10) = 1.59$, $r_{34\to67}(10) = 5.60$, $r_{35\to84}(10) = 1.59$ $r_{39\to68}(10) = 1.02$, $r_{39\to64}(10) = 0.57$, $r_{48\to13}(10) = 1.59$, $r_{51\to99}(10) = 3.41$, $r_{51\to35}(10) = 1.59$, $r_{51\to20}(10) = 2.20$ $r_{64\to13}(10) = 1.59$, $r_{67\to76}(10) = 3.46$, $r_{67\to48}(10) = 1.59$, $r_{67\to13}(10) = 0.56$, $r_{68\to64}(10) = 1.02$, $r_{76\to56}(10) = 3.46$ $r_{84\to87}(10) = 1.59$, $r_{87\to28}(10) = 1.59$, $r_{99\to34}(10) = 2.04$, $r_{99\to6}(10) = 3.56$

[12] C. Jiang, Y. Shi, Y.T. Hou, and W. Lou, "Cherish every Joule: Maximizing throughput with an eye on network-wide energy consumption," in *Proc. IEEE INFOCOM*, pp. 1934–1941, Orlando, Florida, March 25–30, 2012.

[13] M. Kodialam and T. Nandagopal, "Characterizing achievable rates in multi-hop wireless mesh networks with orthogonal channels," *IEEE/ACM Trans. on Networking*, vol. 13, no. 4, pp. 868–880, August 2005.

[14] L. Lin, X. Lin, and N.B. Shroff, "Low-complexity and distributed energy minimization in multihop wireless networks," *IEEE/ACM Trans. on Networking*, vol. 18, no. 2, pp. 501–514, April 2010.

[15] I. Maric and R.D. Yates, "Cooperative multihop broadcast for wireless networks," *IEEE Journal on Selected Areas in Communications*, vol. 22, issue 6, pp. 1080–1088, Aug. 2004.

[16] G.W. Miao, N. Himayat, and G.Y. Li "Energy-efficient link adaptation in frequency-selective channels," *IEEE Trans. on Communications*, vol. 58, no. 2, pp. 545–554, Feb. 2010.

[17] M.J. Neely, "Energy optimal control for time varying wireless networks," *IEEE Trans. on Information Theory*, vol. 52, no. 7, pp. 2915–2934, July 2006.

[18] S. Rosloniec, *Fundamental Numerical Methods for Electrical Engineering*, Springer, Berlin, 2008.

[19] Y. Shi, Y.T. Hou, S. Kompella, and H.D. Sherali, "Maximizing capacity in multi-hop cognitive radio networks under the SINR model," *IEEE Trans. on Mobile Computing*, vol. 10, no. 7, pp. 954–967, July 2011.

[20] J. Tang, G. Xue, C. Chandler, and W. Zhang, "Link scheduling with power control for throughput enhancement in multihop wireless networks," *IEEE Trans. on Vehicular Technology*, vol. 55, no. 3, pp. 733–742, May 2006.

[21] T. Westerlund and F. Pettersson, "An extended cutting plane method for solving convex MINLP problems," *Computers Chem. Eng.*, vol. 19, supplement 1, pp. 131–136, 1995.

[22] J.E. Wieselthier, G.D. Nguyen, and A. Ephremides, "Energy-aware wireless networking with directional antennas: The case of session-based broadcasting and multicasting," *IEEE Trans. on Mobile Computing*, vol. 1, no. 3, pp. 176–192, July–Sept. 2002.

Appendix

Proof of Lemma 2 Our proof is based on contradiction. Assume that the number of linear segments that Algorithm 1 generates is K_l, and $s_l^{(k)}, k = 0, \ldots, K_l$, are the corresponding X-axis values of the endpoints. Suppose that there is another piece-wise linear approximation that needs

$K_l' < K_l$ linear segments and $t_l^{(k)}$s (with $k = 0, \ldots, K_l$, $t_l^{(0)} = 0$ and $t_l^{(K_l')} = s_l^{\max}$) are the corresponding X-axis values of the endpoints.

Since $s_l^{(1)}$ is the largest X-axis value of the second endpoint, we have $t_l^{(1)} \leq s_l^{(1)}$. By induction, we can show that $t_l^{(k)} \leq s_l^{(k)}, k = 1, \ldots, K_l'$. For $k = K_l'$, we have $t_l^{(K_l')} \leq s_l^{(K_l')}$. Further, since $K_l' < K_l$, we also have $s_l^{(K_l')} < s_l^{\max}$. Therefore, we conclude that $t_l^{(K_l')} \leq s_l^{(K_l')} < s_l^{\max}$, which is a contradiction to $t_l^{(K_l')} = s_l^{\max}$. This completes our proof. $\square$

Proof of Lemma 3 Note that the only difference between OPT and OPT-R is the link capacity constraints. Each link capacity constraint for link l in OPT is replaced by a set of linear constraints in OPT-R. Since these linear constraints are generated by the piece-wise linear segments lying beneath the $\log$ curve, the feasible region of OPT-R falls inside in the feasible region of OPT. Thus, a feasible solution to OPT-R is also a feasible solution to OPT. $\square$